



# Growth and characterization of Ce-doped $\text{LiCaAlF}_6$ single crystals

Kiyoshi Shimamura<sup>a,\*</sup>, Na Mujilatu<sup>a</sup>, Kenji Nakano<sup>a</sup>, Sonia L. Baldochi<sup>a</sup>, Zhenlin Liu<sup>b</sup>, Hideyuki Ohtake<sup>b</sup>, Nobuhiko Sarukura<sup>b</sup>, Tsuguo Fukuda<sup>a</sup>

<sup>a</sup> *Institute for Materials Research, Tohoku University, Sendai 980-8577, Japan*

<sup>b</sup> *Institute for Molecular Science, Okazaki 444-8585, Japan*

Received 20 October 1998

## Abstract

Ce-doped  $\text{LiCaAlF}_6$  (Ce : LiCAF) single crystals with high transparency were grown by the Czochralski technique from the stoichiometric composition. A foreign material adhering to the surface of the crystals was investigated. The distribution coefficient of  $\text{Ce}^{3+}$  was determined to be 0.01. Ultraviolet pulse generation with output energy 30.5 mJ and slope efficiency 39% was obtained from a Ce : LiCAF laser. © 1999 Elsevier Science B.V. All rights reserved.

*Keywords:*  $\text{LiCaAlF}_6$ ; Crystal growth; Inclusion; Distribution coefficient; UV laser

## 1. Introduction

Coherent optical sources in the ultraviolet (UV) wavelength region are useful for many practical applications, such as medical procedures, semiconductor processing, micromachining, optical communications and remote sensing [1]. Although various kinds of excimer lasers and tunable color center lasers have been investigated as UV sources, their applications are still restricted because of low-temperature requirements and crystal deterioration or difficulty of safe gas handling. Recently, Ce-doped  $\text{LiCaAlF}_6$  (Ce : LiCAF) crystals have

been reported as leading candidates for UV solid state lasers [2,3]. This matrix can be directly pumped by the fourth harmonic of  $\text{Nd}^{3+}$ -doped  $\text{Y}_3\text{Al}_5\text{O}_{12}$  (Nd : YAG) lasers, and is suitable for tunable all-solid-state lasers in the UV wavelength region.

LiCAF crystals are trigonal with the space group  $P31C$ , and lattice constants  $a = 4.996 \text{ \AA}$  and  $c = 9.636 \text{ \AA}$  [4]. In the past decade, research on LiCAF, and the isostructural matrix  $\text{LiSrAlF}_6$ , mainly concentrated on  $\text{Cr}^{3+}$ -doped crystals, because of their laser operation in the near infrared region. The discovery of their interesting properties, when doped with  $\text{Ce}^{3+}$  ions, for direct UV pumping, stimulated several research groups to investigate the performance of this host as a laser medium in the UV region. However, due to the limited size of

\* Corresponding author. Tel.: + 81 22 215 2103; fax: + 81 22 215 2104; e-mail: shimak@lexus.imr.tohoku.ac.jp.

available crystals, it was difficult to obtain high output energy directly from the Ce : LiCAF laser. Furthermore, the growing of Ce : LiCAF crystals is known to be difficult. A fluorination process using fluorinated gases such as HF [5] is generally necessary in order to purify the raw materials and the growing crystals.

In the present work, we describe the growth of Ce : LiCAF single crystals from the stoichiometric composition by the Czochralski (CZ) technique using powdered raw materials. Problems associated with the crystal growth, such as the presence of foreign substances and scum are investigated. High laser performance was achieved using these Ce : LiCAF crystals.

## 2. Experimental procedure

Crystal growth was performed in a CZ system driven by a 30 KW RF generator. A stoichiometric charge composed of commercially available  $\text{AlF}_3$ ,  $\text{CaF}_2$  and LiF powders, of high purity ( $> 99.99\%$ ), was used as the starting material. As dopants,  $\text{CeF}_3$  and NaF powders of high purity ( $> 99.99\%$ ) were used.  $\text{Ce}^{3+}$  was co-doped with  $\text{Na}^+$  in order to compensate the charge. The concentration of  $\text{Ce}^{3+}$  and  $\text{Na}^+$  in the starting material was in the range of 1–2 mol%. The starting material was placed in a glassy carbon crucible 40 mm in diameter and in height. Growth orientation was controlled by using an  $a$ -axis oriented  $\text{Cr}^{3+}$ -doped LiCAF seed crystal. The pulling rate was 1 mm/h and the rotation rate was 10 rpm.

A vacuum treatment was carried out prior to growth to eliminate water and/or oxygen from the growth chamber and the starting material. The system was heated from room temperature to  $700^\circ\text{C}$  for a period of 12 h under vacuum ( $\approx 10^{-2}$  Torr). Subsequently, high purity Ar gas (99.9999%) was slowly introduced into the furnace. Then, the system was evacuated ( $\approx 10^{-2}$  Torr) and Ar gas was slowly introduced again. Following this treatment the starting material was melted at  $825^\circ\text{C}$ .

Determination of lattice constants and phase identification were performed by X-ray powder diffraction (XRD). The foreign substance present in

the grown crystals was analyzed by electron microprobe analysis. Chemical composition was determined by the induced coupled plasma method. Optical properties of grown crystals were studied by high-resolution FTIR.

## 3. Results and discussion

Fig. 1 shows an as-grown Ce : LiCAF single crystal 20 mm in diameter and 60 mm in length. It is clearly seen that the crystal surface was covered by a large quantity of white foreign material. Fig. 2 shows a wafer from a crystal cut perpendicular to the growth axis and polished. Although the surface of this crystal was covered by the white foreign



Fig. 1. As-grown Ce-doped  $\text{LiCaAlF}_6$  single crystal pulled along the  $a$ -axis.

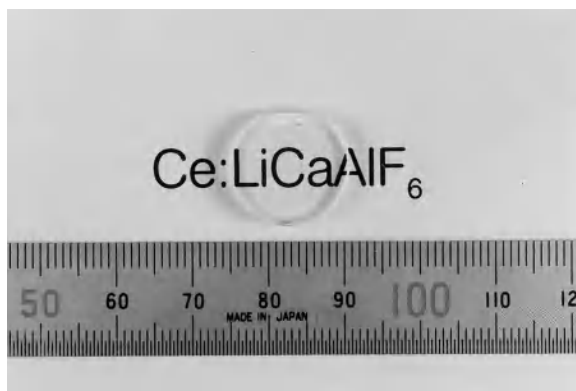


Fig. 2. As-grown wafer cut perpendicular to the growth axis.

material, the bulk of the crystal was transparent without cracks or inclusions. This transparent crystal was identified as a LiCAF single crystal by XRD.

We have grown various LiCAF single crystals with different  $\text{Ce}^{3+}$  and  $\text{Na}^+$  doping levels as shown in Table 1. Although each crystal was transparent and without cracks or inclusions, the crystals were covered by the foreign material as seen in Fig. 1. Although  $\text{Ce}^{3+}$ -doped crystals tended to crack easily,  $\text{Ce}^{3+}$  and  $\text{Na}^+$  co-doped LiCAF and un-doped LiCAF did not. This is probably because of the formation of anion vacancies in order to keep charge neutrality when  $\text{Ce}^{3+}$  is the only dopant.

When the starting material was melted, a black and white scum floating on the melt was observed. Phase identification showed that this scum is composed of carbon, carbon fluoride and oxyfluoride compounds, such as  $\text{Al}_4\text{LiO}_6\text{F}$  and  $\text{CeOF}$ . The carbon may come from the crucible, and/or the raw material, especially from  $\text{AlF}_3$ . Since LiF and  $\text{CaF}_2$  single crystals could be grown without any carbon-containing scum under the same conditions as  $\text{Ce}:\text{LiCAF}$  crystals, the likely source of carbon seems to be  $\text{AlF}_3$ . The oxyfluoride formation may be due to the presence of oxygen or moisture in the system. When these oxygen sources meet fluoride materials, the scum can be formed as oxyfluorides. We tried to remove the scum by scraping after solidifying the melt prior to crystal growth, how-

ever, after further vacuum treatment and remelting, new scum was formed.

Fig. 3a shows a SEM image taken of the foreign material on the crystal surface. This material was confined to an outer layer of thickness approximately  $200\ \mu\text{m}$ . It consisted mainly of volatile fluorides such as  $\text{LiAlF}_4$ , and a small amount of  $\text{AlF}_3$  and  $\text{LiF}$ .  $\text{CaF}_2$  was also detected. The presence of oxides and oxyfluorides such as  $\text{Al}_2\text{O}_3$ ,  $\text{Al}_4\text{LiO}_6\text{F}$  and  $\text{CeOF}$  was recognized as well. Fig. 3b shows a SEM image of a spherical inclusion close to the surface. Such spherical inclusions had the same composition as surface layer. No inclusions other than these spherical ones were detected.

The formation of these foreign substances may have two causes. One is evaporation of the melt

Table 1  
Distribution coefficient of  $\text{Ce}^{3+}$  in  $\text{LiCaAlF}_6$  single crystals and lattice constants of grown crystals

Dopant concentration (mol%)	Distribution coefficient	Lattice constant ( $\text{\AA}$ )
Undoped	–	$a = 4.9942$ $c = 9.5764$
$\text{CeF}_3$ : 1 mol%	$k_{\text{Ce}} = 0.0121$	$a = 4.9808$ $c = 9.6052$
$\text{CeF}_3$ : 1 mol% $\text{NaF}$ : 1 mol%	$k_{\text{Ce}} = 0.0122$	$a = 5.0027$ $c = 9.5768$
$\text{CeF}_3$ : 1.5 mol% $\text{NaF}$ : 1.5 mol%	$k_{\text{Ce}} = 0.00912$	$a = 5.0034$ $c = 9.5981$
$\text{CeF}_3$ : 2 mol% $\text{NaF}$ : 2 mol%	Not measured	$a = 5.0059$ $c = 9.6345$

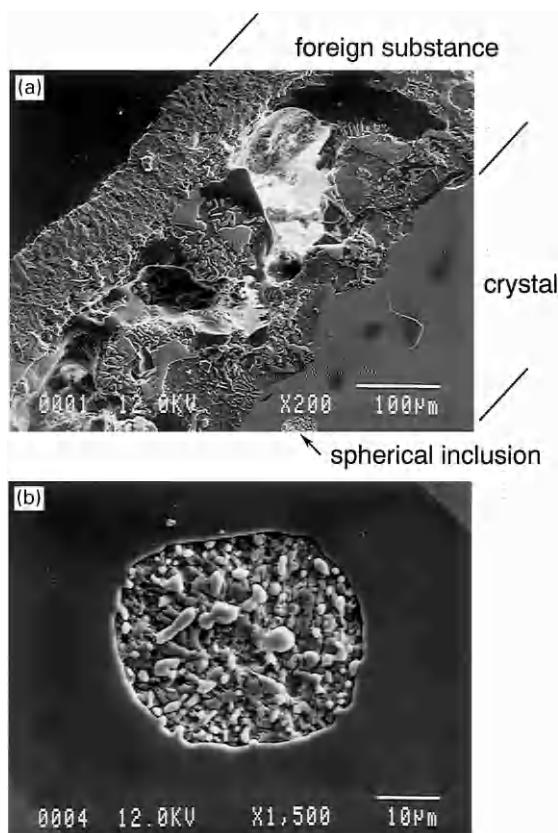


Fig. 3. SEM images of (a) a cross-section of the as-grown crystal with foreign substances on the crystal surface, and (b) a spherical inclusion observed close to the grown crystal surface.

components. Since the vapor pressure ( $p$ ) of  $\text{LiAlF}_4$  is fairly high ( $p_{\text{LiAlF}_4} \approx 1$  Torr at  $800^\circ\text{C}$  [6]),  $\text{LiAlF}_4$  vaporizes continuously and accumulates at the crystal surface during growth.  $\text{AlF}_3$  and  $\text{LiF}$  also have relatively high-vapor pressures ( $p_{\text{AlF}_3}$  and  $p_{\text{LiF}}$  are approximately  $10^{-3}$ – $10^{-2}$  Torr at  $800^\circ\text{C}$  [6]) and behave similarly. The evaporation of the above melt components would shift the melt composition toward the  $\text{CaF}_2$ -rich direction. The excess  $\text{CaF}_2$  in the melt would then aggregate and stick to the growing crystal surface, adding to the foreign material there.

Another cause could be oxide or oxyfluoride formation in the melt because of the presence of water and oxygen in the system or in the raw materials. Since these compounds cannot dissolve into the fluoride melt once they are formed, they float on the melt surface. They could also aggregate, stick to the crystal surface, and form the foreign surface layer.

The above results suggest that the vacuum treatment performed before crystal growth was not sufficient to eliminate contamination derived from water and/or oxygen. Fluoride materials are very sensitive to contamination with water and/or oxygen, and the presence of even a trace amount of oxygen can lead to the formation of  $\text{OH}^-$  and  $\text{OF}^-$  based substances.

The  $\text{Ce}^{3+}$  doping level in the grown crystals was measured, and the distribution coefficient of  $\text{Ce}^{3+}$  ( $k_{\text{Ce}}$ ) in  $\text{LiCAF}$  was estimated as 0.01 (Table 1).  $\text{CeOF}$  formation as a foreign substance could be one reason for the small value of  $k_{\text{Ce}}$ . Lattice constants measured for each crystal are also listed in Table 1. Lattice constants increased depending on the concentration of  $\text{Ce}^{3+}$  and  $\text{Na}^+$ . This is because the ionic radii of  $\text{Ce}^{3+}$  (1.01 Å) and  $\text{Na}^+$  (1.02) are larger than those of  $\text{Li}^+$  (0.76),  $\text{Ca}^{2+}$  (1.00) and  $\text{Al}^{3+}$  (0.535) when the coordination number of  $\text{F}^-$  is 6 [7].

It is known that the existence of  $\text{OH}^-$  degrades laser performance. An absorption peak is observed around  $3620\text{ cm}^{-1}$  when  $\text{OH}^-$  ions exist in the grown crystal [8,9]. Fig. 4 shows the transmission spectrum of our crystals in the infrared wavelength region. Since no absorption peaks are observed around  $3620\text{ cm}^{-1}$ , the crystals do not contain a significant amount of  $\text{OH}^-$ . Although, we did not

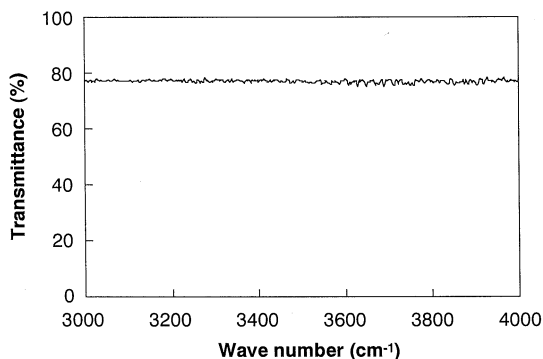


Fig. 4. Transmission spectrum in the infrared wavelength region. The  $\text{OH}^-$  absorption at  $3620\text{ cm}^{-1}$  is negligible.

use an HF atmosphere, as conventionally done to prevent the formation of foreign substances and the evaporation of volatile fluorides, it appears that the oxides and oxyfluorides segregate and end up on the crystal surface. This process seems to exclude  $\text{OH}^-$  from the melt and the bulk of the grown crystals.

The as-grown  $\text{Ce,Na}:\text{LiCAF}$  crystals were colorless. Absorption and fluorescence spectra in the ultraviolet were measured for samples cut from the constant diameter section of crystals. The typical absorption band of  $\text{Ce}^{3+}$  was observed around 270 nm. Therefore,  $\text{Ce,Na}:\text{LiCAF}$  single crystals can be directly pumped by the fourth harmonic of a  $\text{Nd}:\text{YAG}$  laser (266 nm). The fluorescence spectrum showed two bands: one sharp peak at 287 nm and a very broad one near 314 nm. Their intensities were dependent on the  $\text{Ce}^{3+}$  concentration.

Samples from the central part of the grown crystals were used in preliminary tests of laser operation. A schematic diagram of the  $\text{Ce}:\text{LiCAF}$  laser resonator is shown in Fig. 5. The  $\text{Ce}:\text{LiCAF}$  crystal is located between the two cavity mirrors. There is no coating on the parallel end faces of the crystal, which are perpendicular to the optical axis of the resonator. The fourth harmonic of a  $Q$ -switched  $\text{Nd}:\text{YAG}$  laser with a repetition rate of 10 Hz is used as the pumping source. Fig. 6 shows the output energies obtained at 289 nm as a function of the absorbed pump energy at 266 nm. Output energies as high as 30.5 mJ were obtained with a slope

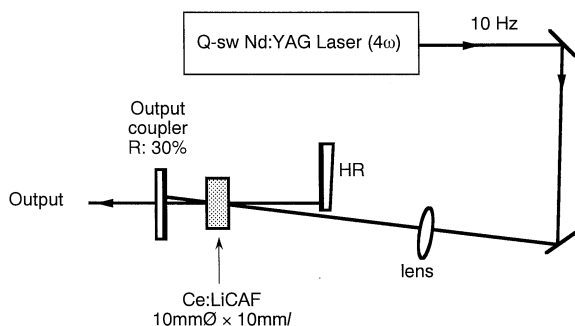


Fig. 5. Experimental setup of a high-energy Ce : LiCAF laser.

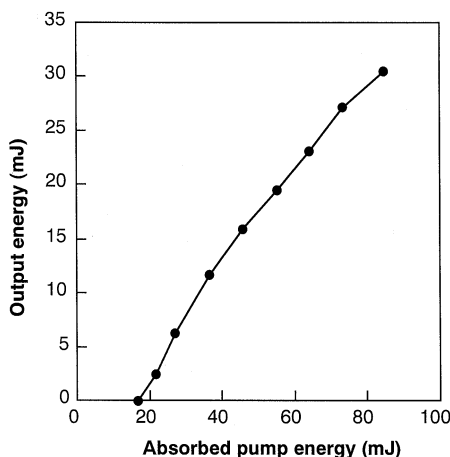


Fig. 6. Laser output energy as a function of absorbed pump energy in a Ce : LiCaAlF<sub>6</sub> sample.

efficiency of 39%. To the author's knowledge, this performance is the highest ever reported for Ce : LiCAF crystals.

#### 4. Summary

Ce : LiCaAlF<sub>6</sub> single crystals were grown by the CZ technique directly from powdered raw materials. Although the crystals were covered by a layer of foreign materials composed of volatile fluorides and oxyfluorides, transparent crystals without cracks and inclusions were obtained. The for-

mation of the foreign material was attributed to vaporization of volatile melt components and to moisture in the growth chamber and in raw materials. The distribution coefficient of Ce<sup>3+</sup> was determined to be 0.01. Lattice constants of LiCAF crystals increased depending on the concentration of Ce<sup>3+</sup> and Na<sup>+</sup>. The laser performance obtained by using the grown crystals shows that Ce : LiCAF is a promising material for high-energy UV pulse generation.

#### Acknowledgements

The authors would like to express sincere thanks to Visiting Professor O. Oda (Japan Energy Corporation) and Associate Professor S. Durbin of the Institute for Materials Research, Tohoku University, for their critical reading of the manuscript and fruitful discussions. The authors are also indebted to Mr. Y. Murakami of the Institute for Materials Research, Tohoku University, for his help in carrying out the chemical composition analysis.

#### References

- [1] N. Sarukura, M.A. Dubinskii, Z. Liu, V.V. Semashko, A.K. Naumov, S.L. Korableva, R.Y. Abdulsabirov, K. Edamatsu, Y. Suzuki, T. Itoh, Y. Segawa, IEEE J. Selected Topics Quantum Electron. 1 (1995) 792.
- [2] M.A. Dubinskii, V.V. Semashko, A.K. Naumov, R.Y. Abdulsabirov, S.L. Korableva, Laser Phys. 3 (1993) 216.
- [3] C.D. Marshall, S.A. Payne, J.A. Speth, W.F. Krupke, G.J. Quarles, V. Castillo, B.H.T. Chai, J. Opt. Soc. Am. B 11 (1994) 2054.
- [4] P. Beaud, M.C. Richardson, Y.-F. Chen, B.H.T. Chai, IEEE J. Quantum Electron. 30 (1994) 1259.
- [5] R.F. Belt, R. Uhrin, J. Crystal Growth 109 (1991) 340.
- [6] D. Klimm, P. Reiche, Proc. Int. Symp. on Laser and Non-linear Optical Materials, 3–5 November 1997, p. 284.
- [7] R.D. Shannon, Acta Crystallogr. A 32 (1976) 751.
- [8] I.M. Ranieri, S.L. Baldochi, A.M.E. Santo, L. Gomes, L.C. Courrol, L.V.G. Tarelho, W. de Rossi, J.R. Berretta, F.E. Costa, G.E.C. Nogueira, N.U. Wetter, D.M. Zzell, N.D. Vieira Jr., S.P. Morato, J. Crystal Growth 166 (1996) 423.
- [9] S.P. Morato, L.C. Courrol, L. Gomes, V. Kalinov, A. Shadarevich, Phys. Stat. Sol. 163 (1991) K61.